Dissociative diffusion of ^{57}Fe in β-Sn as observed by Mössbauer effect

M. Shimotomai
Department of Materials Science, University of Tokyo, Tokyo, Japan

R. R. Hasiguti
Faculty of Engineering, Science University of Tokyo, Kagurazaka, Tokyo, Japan

S. Umeyama
Institute of Industrial Science, University of Tokyo, Tokyo, Japan

(Received 26 July 1976; revised manuscript received 9 May 1977)

The Mössbauer effect of ^{57}Fe atoms in β-Sn was measured over the temperature range 90–462°K with a polycrystalline source specimen. The spectra were decomposed into two major pairs of doublet lines and a minor line. The results were interpreted in terms of a dissociative diffusion mechanism. The lines were assigned to interstitial, substitutional, and clustered ^{57}Fe atoms. The diffusional broadening gave the diffusion coefficient of interstitial Fe atoms along the c axis as $D_i = 1.8(\pm 0.6) \times 10^{-4} \exp[-0.47(\pm 0.07)/kT]$. The effective solute diffusivity comparable with a tracer diffusion coefficient turned out to be $D_I = 4.8(\pm 3.4) \times 10^{-4} \exp[-0.53(\pm 0.08)/kT]$.

I. INTRODUCTION

An increasing number of examples of "fast" impurity diffusion have been reported. Several review papers[1-3] have been published on this subject. The vast majority of the measurements on the fast diffusion have been carried out with a noble or a late transition metal such as Fe, Co, or Ni as solute and Pb, Sn, In, Tl, or alkali metals as host. The phenomena have been interpreted in terms of a dissociative interstitial dissolution and diffusion mechanism proposed by Frank and Turnbull.[4] This mechanism implies that an equilibrium is maintained between the concentration of interstitial solute atoms C_i and that of substitutional solute atoms C_s,

$$\begin{array}{c} C_s \rightleftarrows C_i + C_v \\ \updownarrow \\ VS. \end{array} \qquad (1)$$

Here C_v denotes the vacancy concentration and VS stands for vacancy sources and sinks, The total solute diffusivity D_I is given by

$$D_I = [C_i/(C_i + C_s)]D_i + [C_s/(C_i + C_s)]D_s, \qquad (2)$$

where D_i and D_s are the diffusion coefficients of interstitial and substitutional solute atoms, respectively.

A consideration of valence and size effect led Anthony[2] to postulate the following three criteria for rapid diffusion: (a) a polyvalent or very electropositive solvent, (b) a sufficiently small solute ion size, and (c) a low solute valence. Mundy and McFall[5] summarized the characteristic features common to all the fast diffusers as follows: Independent of whether the host lattice has a close packed or open structure or is multivalent, the values of the activation energy for impurity diffusion are significantly lower than the activation energy for self-diffusion in the host lattice, and the values of the preexponential factor for impurity diffusion are significantly lower than those for self-diffusion. The diffusion parameters for various solutes in single crystals of β-Sn are summarized in Table I. The noble metals[6,7] and[8] Zn have large diffusivities, a few orders of magnitude greater than that for self-diffusion, and they exhibit very striking anisotropy favoring migration along the c axis. As for the diffusion of Co in Sn, the solute satisfies Anthony's three criteria, and the relatively large diffusivity[9] tempts one to classify Co as a fast diffuser. The low values of the diffusivity of Sb,[8] Cd,[8] In,[10] and Hg,[11] have been interpreted as due to substitutional dissolution and a vacancy mechanism. For self-diffusion[12,13] the vacancy mechanism has been supported by high-pressure experiments measuring the activation volume.[14]

It seems difficult to get direct evidence for the supposed dissociative dissolution and interstitial diffusion mechanism with a macroscopic tool such as the tracer-sectioning method. The question of the distribution of the solute atoms between interstitial sites and substitutional sites remains open. The configuration of the interstitial sites is not yet determined conclusively. Miller *et al.*[15] applied a channeling and backscattering technique to obtain the equilibrium fractions of interstitial and substitutional Au atoms dissolved in Sn. They estimated that 95% or more of the Au atoms in Sn at 217 °C were substitutional.

The Mössbauer effect has proved to be a power-

TABLE I. Diffusion parameters for self-diffusion and impurity diffusion in Sn.

Element	Axis	D_0 (cm^2/sec)	Q (eV)	Ref.
Cu	c	$D=2\times10^{-6}$ cm^2/sec at 25 °C		6
	a	2.4×10^{-3}	0.343	
Au	c	5.8×10^{-3}	0.477	7
	a	1.6×10^{-1}	0.768	
Ag	c	7.1×10^{-3}	0.534	7
	a	1.8×10^{-1}	0.798	
Zn	c	1.1×10^{-2}	0.521	8
	a	8.4	0.924	
Co	unspecified	5.5	0.95	9
Hg	c	7.5	1.10	11
	a	3.0×10	1.16	
In	c	1.2×10	1.11	10
	a	3.4×10	1.12	
Sb	c	7.10×10	1.26	8
	a	7.30×10	1.28	
Cd	c	2.20×10^2	1.22	8
	a	1.20×10^2	1.20	
Sn	c	1.28×10	1.13	8
	a	2.10×10	1.12	
Sn	c	8.2	1.11	12
	a	1.4	1.01	
Sn	c	7.7	1.11	13
	a	1.07×10	1.09	

ful technique for the direct observation of the diffusion process on an atomic scale and a time scale of order τ_D, the relaxation time for diffusive jumps of Mössbauer atoms, as well as a tool for studying the electronic and vibrational properties of Mössbauer atoms, embedded in the host. Concerning ^{57}Co or its daughter ^{57}Fe atoms, the interstitial dissolution is inferred, wholly or partially, in In,[16] Te,[17] Si,[18] Ge,[18] and diamond.[19] The dynamic motion of diffusing ^{57}Fe atoms has been observed in Cu,[20] Au,[21] Fe,[22,23] Ti,[24] and Al,[25] by the Mössbauer effect. The atomic motion of the Mössbauer nuclei manifests itself as the broadening of the resonance line. The broadening is described by the self-correlation function formulated by Singwi and Sjölander.[26] The Debye-Waller factor[27,28] (DWF), the isomer shift,[27,29] and the linewidth[30] of ^{57}Fe in β-Sn have been studied by the Mössbauer effect.

The present study is concerned with the diffusion of ^{57}Fe atoms in β-Sn studied by the Mössbauer effect with a view to clarify the mechanism of the diffusion together with the electronic and vibrational properties of the solute in the host lattice.

II. EXPERIMENTS

A polycrystalline Sn foil of 0.25 mm thickness and 99.9995% purity, obtained from Materials Research Corp., was chemically etched and then annealed at 200 °C *in vacuo* to serve as a material for the electrodeposition of ^{57}Co. The electrolyte was an aqueous solution of carrier-free $^{57}CoCl_2$, boric acid, and hydrazine hydrate. A Pt wire was used for the anode. The temperature of the electrolyte was about room temperature (RT). After the electrodeposition of the radioisotope the specimen was rinsed in acetone, dried, and transferred to a glass capsule. It was evacuated to less than 10^{-2} Torr and partially back-filled with hydrogen. Freshly cut Li chips were placed inside the capsule as a getter for any residual oxygen and water vapor. The specimen was then subjected to diffusion annealing at 150 °C. The Mössbauer spectrum taken after 1-h annealing showed a central solid solution line and magnetically split lines ascribable to a Co-rich surface layer. The area intensity of the solid solution line was nearly equal to that of the sextet. Another 2-h annealing decreased the intensity of the latter and increased that of the former remarkably. Finally, the specimen was chemically etched slightly to remove the residual sextet. The activity of the source specimen turned out to be 1.4 mCi. This value is equivalent to a concentration of less than 0.01 at.% of ^{57}Co in the diffused layer.

The spectrometer was a product of Hitachi Works Inc., and was equipped with a 400 channel analyzer working in a constant velocity mode. The experimental setup was horizontal in the transmission geometry with a vibrating source in a small furnace and with an absorber of enriched $K_4Fe(CN)_6\cdot 3H_2O$ at RT except the measurements at 90 °K where the vertical setup was adopted. The linewidth of the absorber itself was estimated to be 0.15 mm/sec. Mössbauer spectra were recorded at seven points over the temperature range 90–462 °K. The accumulated counts per channel were about 5×10^4–6×10^4.

III. RESULTS

The spectra are shown in Figs. 1 and 2. The Mössbauer dips were analyzed by an iterative least-square method assuming lines of Lorentzian shape of independent position, linewidth, and intensity. As the initial attempts, we performed computer fitting of each spectrum with three-line and four-line models, based on the inspection of the resonance patterns. It should be remarked here that we tried about 50 sets of initial parameters on each spectrum to find the best fit since a local minimum of least-squares error was liable to be attained due to the large covariance of the parameters. The quality of the fit of the data to the theoretical curves was tested by computing the values of $\chi^2/\langle\chi^2\rangle$, defined in the usual way. The values are tabulated in Table II. It is clear that the three-line model gave a poor fit. Moreover, the consistency of the decomposition among the spectra was found

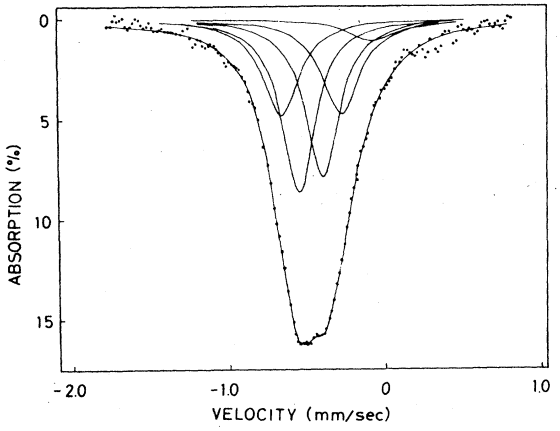

FIG. 1. Mössbauer spectrum taken at room temperature. Solid lines represent the computer-resolved five lines.

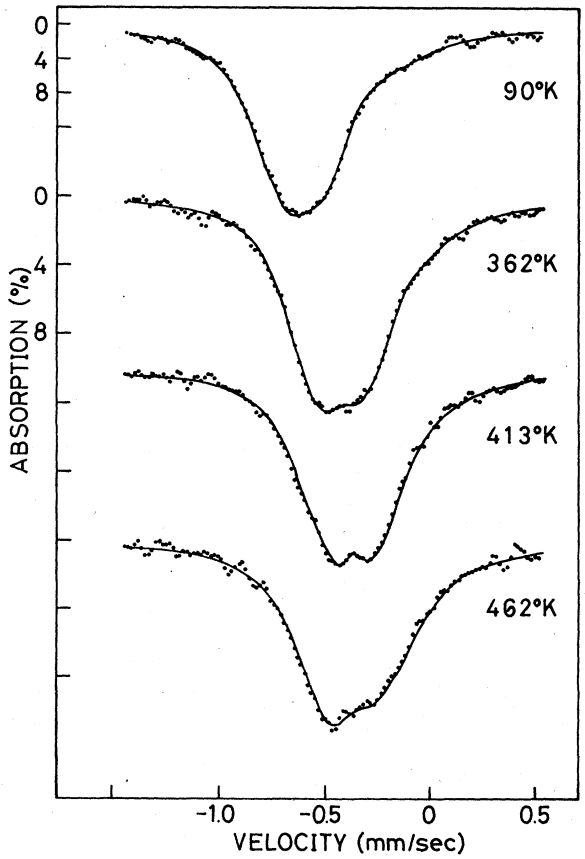

FIG. 2. Mössbauer spectra obtained at several temperatures. Solid lines are the calculated theoretical curves.

to be very bad with this model. The general trends with the four-line model were as follows: (a) the fitting was much improved compared to the three-line model, (b) the two outer lines increased in width and relative intensity with temperature, (c) the widths of the inner lines were approximately equal and remained nearly constant against temperature, and (d) the width of the line at the most positive position was exceptionally broad.

Due to the large anisotropy of a β-Sn lattice (axial ratio, $c/a = 0.546$) one might expect that Fe atoms in a solid solution would manifest themselves as quadrupole-split doublet lines with equal widths. This idea motivated the second step of the analysis. The spectra were fitted with an outer doublet and an inner doublet (width-constrained four-line model). Table II shows that this model is generally between the unconstrained three-line and four-line models in regard to the quality of fit. Close inspection of the data and the theoretical curves, however, has suggested a small additional line at the high velocity region of the dips. This represents the final model. The values of $\chi^2/\langle\chi^2\rangle$ for this five-line model are shown in Table II. The values of parameters determined with this model are physically allowable and the self-consistency of the decomposition is gratifying. The resolved lines for RT spectrum are represented by continuous curves in Fig. 1. Only the total theoretical curves are drawn in Fig. 2 for the sake of clarity. In the following, we shall indicate the five lines as Nos. 1, 2, 3, 4, and 5 in order of increasing velocity. In Fig. 3 the location of the lines are plotted against temperature. The widths of the lines change with temperature as shown in Fig. 4. Figure

TABLE II. Values of $\chi^2/\langle\chi^2\rangle$ for several decomposition models. Lines of Lorentzian shape of independent position, intensity, and width are assumed except where otherwise stated.

Model	90 °K	293 °K	362 °K	387 °K	413 °K	438 °K	462 °K
3 lines	1.311	1.338	1.428	1.770	1.536	1.251	1.164
4 lines	1.491	1.128	1.404	1.572	1.323	1.227	1.158
Width-constrained 4 lines	1.782	1.233	1.644	1.770	1.428	1.293	1.188
Width-constrained 5 lines	1.290	1.080	1.254	1.455	1.299	1.083	1.146

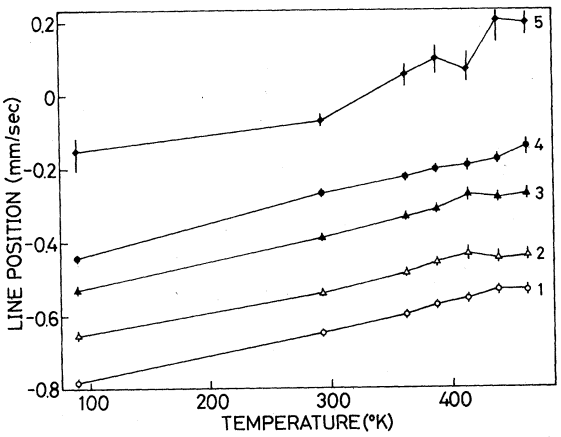

FIG. 3. Location of the five lines as a function of temperature. The five lines are indicated as 1, 2, 3, 4, and 5 in order of increasing volocity. The absorber is enriched $K_4Fe(CN)_6 \cdot 3H_2O$.

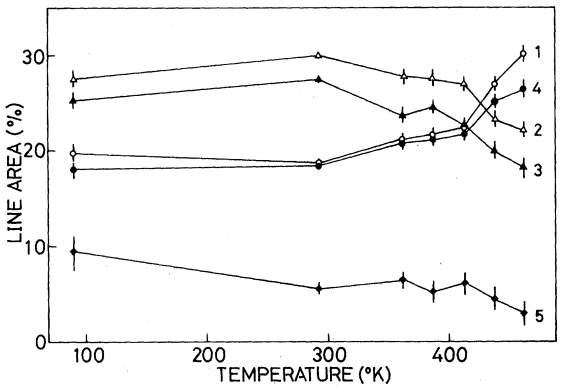

FIG. 5. Relative area intensity of lines as a function of temperature.

5 shows the relative area intensity of the lines as a function of temperature. The analysis errors are indicated in the figures. In Fig. 4, however, the error limits denote the sum of the fitting error and the experimental error caused by the drift of velocity scale over the series of measurements.

These results lead to the following remarks: (i) The similarity of the temperature-dependent characteristics of Nos. 1 and 4 confirms that they are partners of a doublet (1-4 doublet). The same applies to Nos. 2 and 3 (2-3 doublet). The two doublets are dominant in intensity. (ii) The relative area intensity of the 1-4 doublet increases with temperature, while that of the 2-3 doublet decreases. (iii) The linewidth of the 1-4 doublet increases with temperature, while that of the 2-3 doublet remains nearly constant. (iv) The asymmetry of line intensity develops with temperature for both doublets. (v) The isomer shifts of the two doublets are almost the same within the experimental error. There is no remarkable temperature dependence of the quadrupole splitting for both doublets. (vi) Line No. 5 is of a different character in view of its most positive shift, broad width, and small intensity compared to the other lines.

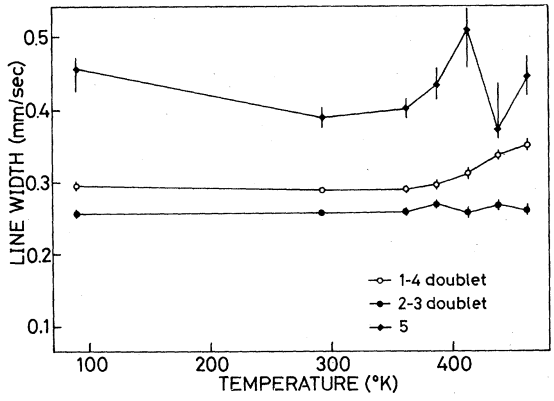

FIG. 4. Temperature dependence of the linewidth.

IV. INTERPRETATIONS AND DISCUSSION

The present experiments have shown that there exist three types of ^{57}Fe atoms in Sn revealing themselves as the 1-4 doublet, the 2-3 doublet, and No. 5. The results can be well explained in terms of a dissociative interstitial dissolution and diffusion mechanism on the following grounds: (a) the fact that the majority of Fe atoms are in two configurations is in accordance with the proposed mechanism, (b) the increase of the 1-4 doublet intensity and the decrease of the 2-3 doublet intensity with temperature are consistent with the prediction of dissociative dissolution as expressed by Eq. (1), and (c) the line broadening of the 1-4 doublet at high temperatures may be attributed to diffusional broadening of interstitial ^{57}Fe atoms. Consequently, the 1-4 doublet and the 2-3 doublet are identified as due to interstitial atoms and substitutional atoms, respectively. Line No. 5 is weak and decays at high temperature. This line may be interpreted as due to clustered Fe atoms. It is known that the clusters of Fe atoms in[31] Cu and[32] Au reveal themselves as doublet lines. In the present case the doublet is not resolved, presumably due to the distribution of the cluster size.

The discussions below will elucidate the above points and clarify the features of the interstitial Fe atoms and substitutional Fe atoms in a Sn lattice.

A. Debye-Waller factor and distribution of Fe atoms

In the source experiments the area of the Mössbauer dip is proportional to DWF and the number of resonantly emitting nuclei.[33] According to the Debye model, DWF is given as

$$f = \exp\left\{-\frac{3E_R}{2k\Theta}\left[1+4\left(\frac{T}{\Theta}\right)^2\int_0^{\Theta/T}\frac{x\,dx}{e^x-1}\right]\right\}, \qquad (3)$$

where E_R is the recoil energy of an unbound emitting nucleus, k is the Boltzmann constant, and Θ is the Debye temperature. The Debye-integral function in the expression has been tabulated.[34] For the fixed geometry of the experimental setup, the ratio of the background corrected area under resonance at different temperatures makes it possible to estimate the Debye temperature. In the present case, however, the number of nuclei giving rise to the 1-4 doublet or the 2-3 doublet is dependent on temperature through a dissociative interstitial dissolution mechanism. The Debye temperatures have been estimated as follows: If one assumes the number of atoms converted to interstitial atoms from substitutional atoms at a certain temperature, one can evaluate the characteristic temperature for each configuration. Therefore, for one conversion rate, a set of the Debye temperatures is determined. Next, for each set, DWF's at RT are evaluated with Eq. (3) and are averaged over the absorption areas. This average DWF is under constraint of being equal to the reported DWF's of ^{57}Fe in Sn,[27,29] determined on the assumption of a single broad solid solution line. The clustered atoms were assumed to be uninvolved in the conversion. The Debye temperature has turned out to be 275 ± 20 °K for the interstitials, 400 ± 40 °K for the substitutionals, and 300 ± 50 °K for the clustered atoms. The experimental data at RT and 387 °K were used for this estimation.

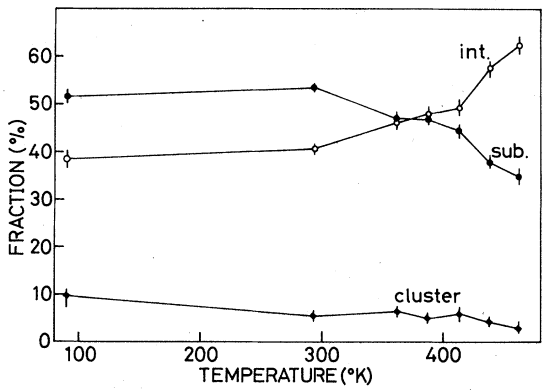

FIG. 6. Fraction of substitutional, interstitial, and clustered Fe atoms as a function of temperature.

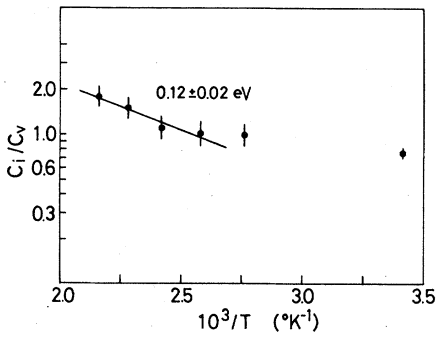

FIG. 7. Population ratio of interstitial Fe atoms to substitutional Fe atoms vs reciprocal temperature.

The values of DWF calculated with Eq. (3) for three types of Fe atoms are used to convert area fraction into concentration fraction. Figure 6 shows the temperature dependence of the Fe atom distribution among the three configurations. It is seen that 54% of Fe atoms are in a substitutional state and that 40% are in an interstitial state at RT. The distribution ratio of the interstitials to the substitutionals is plotted against reciprocal temperature in Fig. 7. The value 0.12 ± 0.02 eV, obtained from the slope, denotes the difference of the formation energy of an interstitial Fe atom and that of a substitutional Fe atom. From Fig. 6 it is derived that the fraction of the interstitials obeys the relation

$$\frac{C_i}{C_i + C_s} = 2.6(\pm 1.2)\exp\left(\frac{-0.06(\pm 0.01)}{kT}\right). \qquad (4)$$

The effective Debye temperature of a substitutional impurity is roughly related to the Debye temperature of the host by

$$\Theta_{\text{eff}} = (M/M')^{1/2}(\gamma'/\gamma)^{1/2}\Theta\,, \qquad (5)$$

where M and M' are the masses of the host atom and the impurity atom, respectively, while γ and γ' are the spring constants of the host-host and the host-impurity binding, respectively.[35] With the Debye temperature 199 °K for Sn, the ratio γ'/γ is calculated to be 1.2. This means that the impurity-host coupling is tighter than the host-host one. The low Debye temperature of the interstitial Fe atoms is noted, since it has been usual to expect a strong force constant for an interstitial atom. The implication of the low value will be discussed in a later section.

It should be noted that the above analyses have been made within the framework of the Debye model. It might be safe to say that an inclusion of anharmonicity would not essentially change the analyses if the extent of the anharmonicity is comparable among three types of Fe atoms.

B. Linewidth and diffusivity

The relationship between the Mössbauer absorption and diffusion in solids was discussed by Singwi and Sjölander,[26] and they formulated the energy distribution of emitted radiation as follows:

$$I(E) \propto \int dt \exp\left(\frac{-i(E-E_0)t}{\hbar}\right) \times \exp\left(\frac{-\Gamma|t|}{2\hbar}\right) G_s(\vec{k}, t), \quad (6)$$

where Γ is the natural width of the excited nuclear level and $\vec{k}$ is the wave vector of the radiation. $G_s(\vec{k}, t)$ is the Fourier transform of the function $G_s(\vec{r}, t)$, which is the self-correlation function describing how often on the average an atom is at position $\vec{r}$ at time t, having begun its motion from $\vec{r}=0$ at $t=0$. In the case of diffusion in solids, an atom is seen to make sudden jumps between identical vibrational states centered at different positions in the lattice. It is also assumed that vibrational motion and diffusional motion are uncorrelated. The result is that the Mössbauer absorption cross section would have a Lorentzian shape with line broadening given by (in energy units)

$$\Delta\epsilon = 2\hbar\tau_D^{-1}[1-\alpha(\vec{k})], \quad (7)$$

where

$$\alpha(\vec{k}) = \int d\vec{r} \exp(i\vec{k}\cdot\vec{r}) h(\vec{r}).$$

The function $h(\vec{r})$ indicates the probability that an atom has moved to a position $\vec{r}$ relative to the origin after one jump. In evaluating $\alpha(\vec{k})$, a crystal structure has to be taken into account. Chudley and Elliott[36] have considered the effect of restricting the jump directions to certain crystallographic directions. β-Sn with a body-centered-tetragonal structure has large rectangular tunnels in the c direction along which interstitial atoms could migrate easily. In the a direction, however, no comparable interstitial channels exist and a migrating interstitial atom would be forced to follow a much more twisting path. In fact, Cu, Au, Ag, and Zn have been observed to diffuse about ten times faster in the c direction than in the a direction (see Table I). Consequently, one might reasonably assume that one would observe diffusional broadening due to the migrating atoms along the c direction. Then $\alpha(\vec{k})$ would be given by

$$\alpha(\vec{k}) = \cos(k_c c), \quad (8)$$

where k_c is the component of the momentum of the radiation referred to the c axis and c is the lattice parameter. If there is no pronounced texture in the specimen, $\alpha(\vec{k})$ is averaged to be approximately nil. For the supposed one-dimensional diffusion,

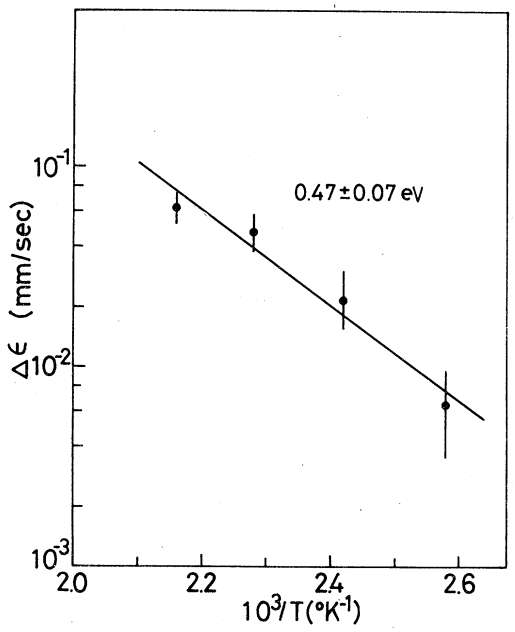

FIG. 8. Line broadening of 1-4 doublet in excess of the room-temperature value. The slope gives the activation energy of diffusion.

the diffusivity D is given by

$$D = \tfrac{1}{2} f_c c^2 \tau_D^{-1}, \quad (9)$$

where f_c is the Bardeen-Herring correlation factor. This factor is unity for a freely migrating interstitial atom. The linewidth of the 1-4 doublet in excess of the value at RT is shown against reciprocal temperature in Fig. 8. With the help of Eqs. (7)–(9) one finds

$$D_i = 1.8(\pm 0.6) \times 10^{-4} \exp[-0.47(\pm 0.07)/kT]. \quad (10)$$

The attempt frequency for jumps is estimated to be 3.7×10^{11} sec^{-1}.

A diffusion constant measured by a tracer-sectioning method is the effective solute diffusivity given by Eq. (2). In the dissociative diffusion one may expect $D_i \gg D_s$ and approximate D_I as $D_i C_i/(C_i + C_s)$. The multiplication of Eq. (4) to Eq. (10) yields

$$D_I = 4.8(\pm 3.4) \times 10^{-4} \exp[-0.53(\pm 0.08)/kT]. \quad (11)$$

The small preexponential factor and the small activation energy represent the features characteristic to fast diffusers.[5] The diffusivities of various elements in β-Sn are shown in Fig. 9 including the present result. The difference between our result and that of a tracer experiment for Co seems to stem from the difference of the diffusion direction and/or the measuring method. It is well-known that the diffusion parameters obtained by the tracer sectioning method is often influenced by

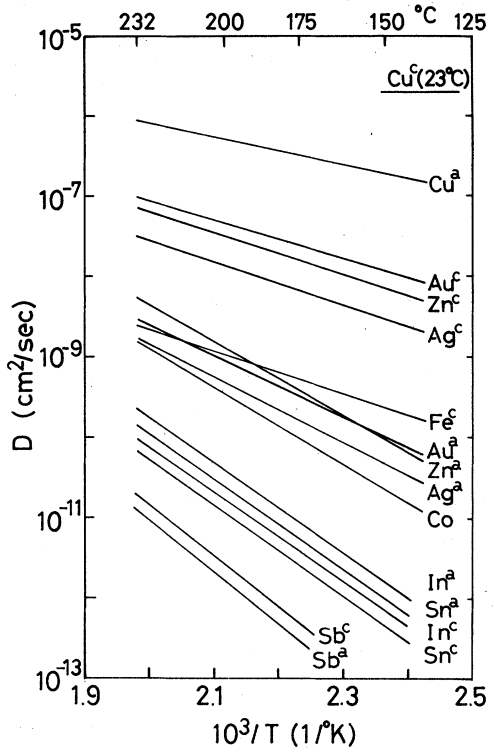

FIG. 9. Diffusion coefficients as a function of temperature for self-diffusion and impurity diffusion in β-Sn. Superscripts a and c denote diffusion along a axis and c axis, respectively.

solution trapping. The overall large linewidth of the 1-4 doublet compared to the 2-3 doublet remains unexplained.

C. Goldanskii-Karyagin effect

Asymmetry in the intensity of the component lines of quadrupole doublets has been observed in the spectra of some polycrystalline materials, particularly in some Sn compounds and has been interpreted by Karyagin[37] and Goldanskii *et al.*[38] as due to the anisotropy of DWF. If DWF is a function of the angle θ between the principal axis of the electric field gradient tensor and the direction of the observation, the asymmetry of the transition from $\frac{3}{2}$ and $\frac{1}{2}$ levels of the excited states, denoted by $I_{3/2}$ and $I_{1/2}$ respectively, in a polycrystallite is given by

$$R=\frac{I_{3/2}}{I_{1/2}}=\int_0^{\pi/2}(1+\cos^2\theta)f(\theta)\sin\theta d\theta \Big/ \int_0^{\pi/2}(\tfrac{5}{3}-\cos^2\theta)f(\theta)\sin\theta d\theta\,, \qquad (12)$$

and differs from unity. Pfannes and Gonser,[39] however, raised the question of the applicability of the Goldanskii-Karyagin effect to a material with texture. They computed the asymmetry in a hyperfine pattern for various orientation distributions and concluded that the influence of texture must be examined before the *ad hoc* assumption of the Goldanskii-Karyagin effect. When the contribution from the preferred orientation is taken account, Eq. (12) is modified to

$$R=\int_0^{\pi/2}(1+\cos^2\theta)f(\theta)D(\theta)\sin\theta d\theta \Big/ \int_0^{\pi/2}(\tfrac{5}{3}-\cos^2\theta)f(\theta)D(\theta)\sin\theta d\theta\,, \qquad (13)$$

where $D(\theta)$ indicates the distribution function of the preferred orientation. It has been assumed that the texture posesses axial symmetry and that the principal axis of the electric field gradient coincides with a crystallographic axis. In the harmonic approximation, $f(\theta)$ is given by[40]

$$f(\theta)=\exp(-\delta\cos^2\theta)\,, \qquad (14)$$

$$\delta=k^2(\langle z^2\rangle-\langle x^2\rangle)\,. \qquad (15)$$

Here δ denotes the vibrational anisotropy in terms of a mean-square displacement of lattice atoms parallel to $\langle z^2\rangle$ and perpendicular $\langle x^2\rangle$ to the principal axis. In Fig. 10 the asymmetry R is plotted as a function of δ for three simple distribution functions: $D(\theta)=1$, $\cos\theta$, and $1-\cos\theta$. These functions are designed to represent random distribution, (001) texture, and (100) texture, respectively.

The theory[41] and experiment[42] on the vibrational anisotropy in β-Sn have revealed that the mean-square displacement in the c direction is larger

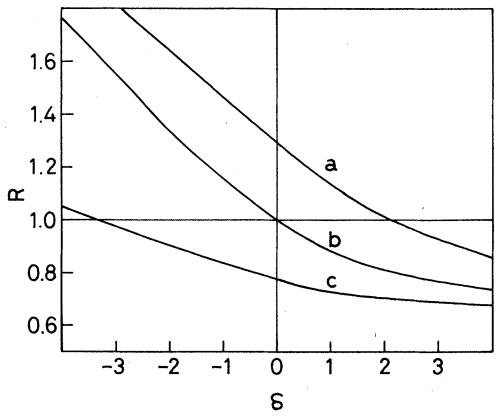

FIG. 10. Line intensity ratio of a doublet R vs lattice anisotropy parameter δ for three crystalline distribution functions $D(\theta)$. $D(\theta)=\cos\theta$ for curve a, $D(\theta)=1$ for curve b, and $D(\theta)=1-\cos\theta$ for curve c represent (001) texture, random texture, and (100) texture, respectively.

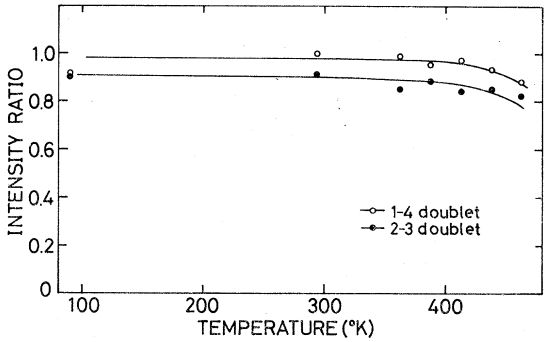

FIG. 11. Intensity ratio of the partner lines for 1-4 doublet and 2-3 doublet as a function of temperature.

than that in the a direction and that the anisotropy becomes more pronounced at high temperatures; $\langle z^2\rangle - \langle x^2\rangle$ in Eq. (15) is positive and increases with temperature. It will be reasonable to presume that an interstitially or substitutionally incorporated Fe atom exhibits anisotropic lattice vibration similar to that exhibited by the host atoms. The intensity ratios of the partner lines for the 1-4 doublet and the 2-3 doublet are shown in Fig. 11 as a function of temperature. Asymmetry evolves with temperature for both doublets. Referring to Fig. 10, one infers that the orientation distribution of the crystallites in the specimen is a little deviated from randomness to (100) texture since δ is expected to be positive and the R values for the doublets fall between curves b and c in the physically plausible range of $\delta = 0-2$. The possibility of (001) texture may be ruled out by the observed development of the asymmetry with δ. Consequently, it is concluded that Nos. 3 and 4 correspond to $\frac{1}{2}$ transition. From these assignments it is deduced that the sign of electric field gradient is plus for both the 1-4 doublet and the 2-3 doublet.

D. Electronic properties

Some assistance in understanding the nature of resonance lines is provided by the discussion of the isomer shift. The isomer shift measures the s- and d-electron densities at ^{57}Fe nucleus. In order to compare the measured shifts in the present study with data taken relative to metallic Fe, we have to add 0.045 mm/sec, the shift of the $K_4Fe(CN)_6 \cdot 3H_2O$ absorber with respect to metallic Fe. At RT the isomer shift is -0.417 ± 0.006 mm/sec for the 1-4 doublet, -0.425 ± 0.006 mm/sec for the 2-3 doublet, and -0.03 ± 0.01 mm/sec for No. 5. We have neglected the contribution from the second-order Doppler shift. The shifts of the doublets are in good agreement with the values -0.395 mm/sec,[29] and -0.45 mm/sec,[27] which were determined by assuming a single but slightly asymmetric solid solution line. The nearly equal shifts for the doublets mean that the electronic binding of ^{57}Fe ions to a Sn lattice is substantially the same. It has been found from the studies on Fe-Sn compounds[43] that the Fe-Sn bond is of an unsaturated covalentlike nature consisting of sp^3 hybrids and that the $3d$ electron population is probably not influenced with bonding. The equal shifts for both the interstitial and the substitutional doublets have been also observed for ^{57}Fe atoms in[17] Te. The shift of No. 5 indicates that the electron density at the nuclei is large compared to that of the other configurations and closer to metallic Fe. This feature supports the assignment of this small line to clusters of ^{57}Fe atoms. The temperature dependence of the line position for the doublets can be interpreted as due to the second order Doppler shift within the experimental error.

The values of the quadrupole splitting are found to be 0.382 ± 0.004 and 0.153 ± 0.004 mm/sec for the 1-4 and the 2-3 doublets, respectively. The electric quadrupole interaction measures the distortion of the iron inner electrons and valence electrons and of the lattice from cubic symmetry. The quadrupole splitting is expressed as

$$E_Q = \tfrac{1}{2} e^2 q Q (1 + \tfrac{1}{3}\eta^2)^{1/2}, \tag{16}$$

where e is the electronic charge, Q is the nuclear quadrupole moment, η denotes the asymmetry parameter, and eq is the field gradient along the principal axis. It is customary to describe the electric field gradients in metals as consisting of a lattice contribution and an electronic contribution

$$eq = (1 - R) eq_{el} + (1 - \gamma_\infty) eq_{lat}. \tag{17}$$

Here eq_{lat} is the field gradient generated by the superposition of the Coulomb fields from lattice point charges corresponding to the ionic cores of the host atoms. The Sternheimer factor $1 - \gamma_\infty$ accounts for the field gradient enhancement at the nucleus due to the polarization of the closed shells which is caused by the crystal field. The term eq_{el} is the contribution from the spatial distribution of all electrons. In the case of ^{57}Fe nucleus the principal contribution comes from the $3d$ electrons of an Fe atom. The factor $1 - R$ accounts for the effect of the polarization of the closed shell electrons by eq_{el}. These contributions cannot be estimated without the knowledge of the site symmetry of the Mössbauer nucleus and the wave functions of electrons. In the present case, however, where the isomer shifts for the two configurations are nearly equal, it might as well be assumed that the difference between the splitting of the two doublets comes mainly from the lattice contribution.

E. Interstitial site

It has been usual to discuss the possibility of interstitial dissolution of an impurity atom by considering the impurity ion size and the diameter of the largest hard sphere that could be accomodated in the lattice. The interstitial dissolution of noble metals in Pb and Sn has been interpreted[1,44] in terms of modified Hägg's rule.[45] A calculation shows that with Sn atoms in +4 ionization states, as is thought to be the case, even a neutral ^{57}Co or its daughter ^{57}Fe atom would fit into a tetrahedral interstitial site.

Huang and Huntington,[8] however, have made a close examination of a Sn lattice and pointed out that the large interstitial tunnels down the c axis possess a screw-axis symmetry of $\frac{2}{4}\pi$. As a result, an impurity atom moving a lattice translational distance c along the tetragonal axis would pass through three intervening tetrahedral positions which are off the screw axis. This means that the effective jump distance in this direction is cut by a factor of 4. They argued that the activation barrier would be reduced by roughly $\frac{1}{16}$ under what one might otherwise expect and would fall in the general range of thermal energies. They ascribed the small activation energy of diffusion along the c axis to the energy necessary to bring the impurity from a substitutional site to an interstitial site. Their finding on the symmetry of the lattice does make it impracticable to assign tetrahedral interstitial sites for interstitial Fe atoms in view of the present results described in Secs. IV A and IV B.

The clue to the question of the interstitial site may be sought in the sign and the magnitude of the electric field gradient. As stated earlier, the sign of the electric field gradient, which is equal to the sign of the quadrupole splitting for ^{57}Fe nuclei, is plus and the difference between the splitting of the interstitial doublet and that of the substitutional doublet is probably dominated by a lattice contribution. The eq_{lat} in Eq. (17) is defined for an array of Sn^{+4} ions by the relation

$$eq_{\mathrm{lat}} = 4e \sum_i \left(\frac{3z_i^2 - r_i^2}{r_i^5} \right). \tag{18}$$

We computed the lattice sum in the expression for various configurations of Fe ions with the general formulas which were devised by de Wette and Schacher.[46] No relaxation around an Fe ion was considered. The antishielding factor $1-\gamma_\infty$ of 12,[47] the nuclear quadrupole moment Q of $0.20b$,[48] and the asymmetry parameter η of 0 were adopted in the evaluation of E_Q given by Eq. (16). The results for a substitutional site, a tetrahedral interstitial site, a bond-centered interstitial site, and split interstitial sites are listed in Table III along with the experimental values. It is clear that a [001] split configuration with an impurity atom and the associated host atom displaced about (20–30)% of the lattice parameter from a regular lattice site, a so called mixed dumbbell configuration, might account for the observed difference of the quadrupole splitting between the 1-4 doublet and the 2-3 doublet.

If this theoretical consideration is correct, the low value of the Debye temperature for interstitial Fe atoms (275 °K) and the small jump attempt frequency (4×10^{11} sec^{-1}) might be understood in terms of the resonance modes which have been established for self-interstitials in the dumbbell configuration in face-centered-cubic metals theoretically[49] and experimentally.[50] The occurrence of low-frequency resonant modes beside high-frequency modes is explained by the strongly compressed lattice around the interstitials. The interstitials are expected to vibrate in the localized modes and the resonant modes but practically not in the normal modes. The attempt frequency for jumps may have relevance to the librational resonance mode. Mixed dumbbell interstitials have been observed in irradiated dilute Al alloys by a channeling technique[51] and by the Mössbauer effect.[52] It is interesting to note that the effect of isotope mass on diffusion of Ag in Sn along the a direction was accounted for by a mixed-dumbbell model.[3]

With a mixed-dumbbell configuration, the activation energy of diffusion in the c direction might be attributed to the energy necessary to dissociate a mixed dumbbell and bring the impurity atom into the channel along the c axis. Another explanation

TABLE III. Theoretical quadrupole splitting due to a point ion lattice for various configurations of an impurity ion. Percentage in the parentheses refers to the displacement of the split atoms from a regular lattice site in each direction. Experimental values are also shown.

	E_Q (mm/sec)
Theoretical (lattice contribution)	
tetrahedral interstitial site	−0.021
bond-centered interstitial site	−0.037
[110] split interstitial site (20%)	−0.008
[111] (20%)	−0.019
[100] (20%)	0.010
[001] (20%)	0.095
[001] (30%)	0.51
substitutional site	−0.016
Experimental	
1-4 doublet (interstitial Fe)	0.382
2-3 doublet (substitutional Fe)	0.153

is possible based on the model of the diffusion of Ag in Pb,[53] a mixed dumbbell might make rotational jumps between the equivalent orientations and subsequently make dissociative jumps. In this case the activation energy of diffusion is related to the process of rotational and dissociative jumps.

V. SUMMARY

We have measured the Mössbauer effect of ^{57}Fe atoms embedded in β-Sn very dilutely and have revealed spectra with a fine structure. The decomposition of spectra with an iterative least-squares method indicated that the majority of Fe atoms were either in a substitutional state or in an interstitial state. The temperature dependence of the distribution of Fe atoms between two configurations was consistent with the prediction of a dissociative interstitial dissolution and diffusion mechanism proposed by Frank and Turnbull. We have found the broadening of the line-width of the interstitial doublet and evaluated the diffusion coefficient from the broadening. It was inferred by assuming similar vibrational anisotropy of the interstitials to that of the host atoms that the interstitial Fe atoms were in a [001] mixed dumbbell configuration. The possible role of the low frequency resonance modes concomitant to the dumbbell interstitials in fast diffusion has been pointed out.

The electronic and vibrational properties of a mixed dumbbell themselves represent a very interesting problem and are worthy of further investigation. It will be fruitful to examine the implication of a mixed dumbell model in the atomic process of diffusive jump and in the isotope effect on diffusion.

ACKNOWLEDGMENTS

The authors appreciate Professor U. Gonser for his discussion on the effect of texture. They wish to express their indebtedness to Y. Koizumi, S. Yamashita, and the other staff members of Radio-Isotope Center of the University of Tokyo for valuable assistance to the experiments.

[1]D. Turnbull, Proceedings of the Memorial Lecture Meeting, National Research Institute of Metals, Tokyo, 1966 (unpublished), p. 1.
[2]T. R. Anthony, *Vacancies and Interstitials in Metals*, edited by A. Seeger et al. (North-Holland, Amsterdam, 1970), p. 935.
[3]W. K. Warburton and D. Turnbull, *Diffusion in Solids; Recent Developments*, edited by A. S. Nowick and J. J. Burton (Academic, New York, 1975), p. 171.
[4]F. C. Frank and D. Turnbull, Phys. Rev. 104, 617 (1956).
[5]J. N. Mundy and W. D. McFall, Phys. Rev. B 8, 5477 (1973).
[6]B. F. Dyson, T. R. Anthony, and D. Turnbull, J. Appl. Phys. 38, 3408 (1967).
[7]B. F. Dyson, J. Appl. Phys. 37, 2375 (1966).
[8]F. H. Huang and H. B. Huntington, Phys. Rev. B 9, 1479 (1974).
[9]W. Chomka and J. Andruszkieicz, Nucleonik 5, 611 (1960).
[10]A. Sawatzky, J. Appl. Phys. 29, 1303 (1958).
[11]W. K. Warburton, Phys. Rev. B 6, 2161 (1972).
[12]J. D. Meakin and E. Klokholm, Trans. AIME 218, 463 (1960).
[13]C. Coston and N. H. Nachtrieb, J. Phys. Chem. 68, 2219 (1964).
[14]K. L. Devnies, G. S. Baker, and P. Gibbs, J. Appl. Phys. 34, 2254 (1963); 34, 2258 (1963).
[15]J. W. Miller, D. S. Gemmell, R. E.Holland, J. C. Poizat, J. N. Worthington, and R. E. Loess, Phys. Rev. B 11, 990 (1975).
[16]P. A. Flinn, U. Gonser, R. W. Grant, and R. M. Housley, Phys. Rev. 157, 530 (1967).
[17]V. Fano and I. Ortalli, Phys. Status Solidi 33, K109 (1969).
[18]G. L. Lastshaw, G. D. Sprouse, P. B. Russell, G. M. Kalvius, and S. S. Hanna, Bull. Am. Phys. Soc. 13, 1949 (1968).
[19]F. de S. Barros, D. Hafemeister, and P. J. Viccaro, J. Chem. Phys. 52, 2865 (1970).
[20]R. C. Knauer and J. G. Mullen, Phys. Rev. 174, 711 (1968).
[21]R. C. Knauer and J. G. Mullen, Appl. Phys. Lett. 13, 150 (1968).
[22]S. J. Lewis and P. A. Flinn, Appl. Phys. Lett. 15, 311 (1969).
[23]R. Lindsey, Phys. Status Solidi B 75, 583 (1976).
[24]S. J. Lewis and P. A. Flinn, Philos. Mag. 26, 977 (1972).
[25]K. Sørensen and G. Trumpy, Phys. Rev. B 7, 1791 (1973).
[26]K. S. Singwi and Sjölander, Phys. Rev. 120, 1093 (1960).
[27]J. Bara and A. Z. Hrynkiewicz, Phys. Status Solidi 15, 205 (1966).
[28]S. M. Qaim, J. Phys. F 1, 320 (1971).
[29]S. M. Qaim, Proc. Phys. Soc. Lond. 90, 1065 (1967).
[30]S. M. Qaim, P. J. Black, and M. J. Evans, J. Phys. C 1, 1388 (1968).
[31]S. J. Campbell, P. E. Calrk, and P. R. Liddell, J. Phys. F 4, 1073 (1974).
[32]B. Window, Phys. Rev. B 6, 2013 (1972).
[33]R. M. Housley, N. E. Erickson, and J. G. Dash, Nucl. Instrum. Methods 35, 77 (1965).
[34]A. H. Compton and S. K. Allison, *X-Rays in Theory and Experiment* (D. Van Nostrand, New York, 1935), p. 437.
[35]W. A. Steyert and R. D. Taylor, Phys. Rev. 133, A1553 (1964).
[36]C. T. Chudley and R. J. Elliot, Proc. Phys. Soc. Lond. 77, 353 (1961).
[37]S. V. Karyagin, Sov. Phys.-Doklady 148, 1102 (1963).
[38]V. I. Goldanskii, G. M. Gorodinski, S. V. Karyagin, L. A. Korytoko, L. M. Krizhanski, E. F. Markorov, and

I. P. Suzdalov, Sov. Phys.-Doklady 147, 127 (1962).
[39]H. D. Pfannes and U. Gonser, Appl. Phys. 1, 93 (1973).
[40]P. A. Flinn, S. L. Ruby, and W. L. Kehl, Science 143, 1434 (1964).
[41]E. G. Brovman and Yu. Kagan, Sov. Phys.-Solid State 8, 1402 (1966).
[42]A. P. Kirianov and N. E. Aledseevskii, *Proceedings of the Conference on Application of the Mössbauer Effect*, edited by I. Dézsi (Akademiai Kiado, Budapest, 1971), p. 261.
[43]G. Trumpy, E. Both, C. Djèga-Marriadassou, and P. Lecocq, Phys. Rev. B 2, 3477 (1970).
[44]T. R. Anthony and D. Turnbull, Phys. Rev. 151, 495 (1966).
[45]G. Hägg, Z. Phys. Chem. B6, 221 (1929); 7, 339 (1930); 8, 445 (1930).
[46]F. W. de Wette and G. F. Schacher, Phys. Rev. 137, A78 (1965).
[47]R. Ingalls, Phys. Rev. 133, A787 (1964).
[48]A. J. Nozik and M. Kaplan, Phys. Rev. 159, 273 (1967).
[49]P. H. Dederichs, C. Lehman, and A. Scholz, Phys. Rev. Lett. 31, 1130 (1973).
[50]J. Holder, A. V. Granato, and L. E. Rehn, Phys. Rev. Lett. 32, 1054 (1974).
[51]M. L. Swanson, Can. J. Phys. 53, 1117 (1975).
[52]G. Vogl, W. Mansel, and P. H. Dederichs, Phys. Rev. Lett. 36, 1497 (1976).
[53]J. W. Miller, J. N. Mundy, L. C. Robinson, and R. E. Loess, Phys. Rev. B 8, 2411 (1973).